American Mineralogist, Volume 84, pages 848–855, 1999

High-temperature heat capacity of grossular ($Ca_3Al_2Si_3O_{12}$), enstatite ($MgSiO_3$), and titanite ($CaTiSiO_5$)

LAURENT THIÉBLOT,* CHRISTOPHE TÉQUI, AND PASCAL RICHET†

Laboratoire de Physique des Géomatériaux, URA CNRS 734, Institut de Physique du Globe 4, place Jussieu, 75252 Paris Cédex 05, France

ABSTRACT

The heat capacities of synthetic grossular ($Ca_3Al_2Si_3O_{12}$), ortho- and protoenstatite ($MgSiO_3$), and titanite ($CaTiSiO_5$) were determined from drop-calorimetry measurements made between 400 K and 1390, 1811, and 1809 K, respectively. The heat capacity of grossular increases smoothly with temperature before leveling off in an anomalous way above 1500 K. For enstatite, no large heat capacity difference seems to occur between the ortho- and protoenstatite forms although important premelting effects are observed for protoenstatite above 1700 K. Our results for titanite up to the melting point confirm the minimal calorimetric effects at the para-antiferroelectric transition near 500 K and the large magnitude of the premelting enthalpy, which represents about 25% of the reported enthalpy of fusion.

INTRODUCTION

In spite of their importance in the lower crust and upper mantle, garnets and enstatites are minerals whose physical properties at high temperatures are not so well known. At 1 bar, for example, calorimetric measurements on well-characterized samples extend up only about 1000 K (e.g., Krupka et al. 1979, 1985; Watanabe 1982; Bosenick et al. 1996).

For garnets, measurements have long been hampered by the fact that these high-pressure minerals are prone to decomposition when heated at 1 bar. Then, the availability of large amounts of an almost pure natural pyrope ($Mg_3Al_2Si_3O_{12}$) made it possible to determine the heat capacity through drop-calorimetry experiments performed to 1340 K (Téqui et al. 1991), i.e., a temperature high enough to make reliable extrapolations to upper mantle conditions. Grossular ($Ca_3Al_2Si_3O_{12}$), the calcic end-member of the aluminosilicate garnets, does not occur naturally in a pure form. However, it is stable at lower pressures than pyrope, which makes synthesis of large quantities possible and suggests that at 1 bar grossular would not decompose at much lower temperatures than pyrope. Actually, the drop-calorimetry measurements reported in this paper could be made up to 1386 K. In addition to obtaining high-temperature data, the new measurements on grossular were motivated by the controversy over the systematic differences between low-temperature heat capacities measured by adiabatic calorimetry and those calculated from spectroscopically derived vibrational density of states (e.g., Hofmeister and Chopelas 1991).

For enstatite, the magnesian end-member orthopyroxene, calorimetric measurements have been hampered by complex polymorphism and difficulties distinguishing the various modifications (e.g., Smith 1969; Smyth 1974; Lee and Heuer 1987). Ortho- and protoenstatite, the polymorphs stable at low and high temperatures, respectively, can be obtained in large amounts, which allowed us to make measurements over wide temperature intervals. In addition to determining how the high-temperature heat capacity of these phases depends on their structure, we also investigated whether protoenstatite shows enthalpy anomalies before melting similar to those already found for other minerals with a pyroxene stoichiometry (Richet and Fiquet 1991).

In addition, we have also redetermined the heat capacity of titanite ($CaTiSiO_5$). This mineral recently has been the subject of several structural investigations (Ghose et al. 1991; Zhang et al. 1995; Chrosch et al. 1997; Xirouchakis et al. 1997a), with a great deal of attention focused on the para-antiferroelectric phase transition near 500 K. On the other hand, the available calorimetric data show large premelting anomalies in the enthalpy beginning about 110 K below the congruent melting temperature (King et al. 1954). Such premelting effects have recently been interpreted as configurational changes in crystals associated with an enhanced mobility of the network modifying cations (Richet et al. 1994, 1998). Interest in titanite thus stems from its much differing stoichiometry with respect to the pyroxene or feldspar minerals investigated previously.

EXPERIMENTAL METHODS

Materials

As described in detail by Thiéblot et al. (1998), which should be consulted for further details, grossular was prepared from a synthetic glass treated hydrothermally at 1070 K and 1.8 kbar in an internally heated vessel. Vacuum fusion analysis and thin-film infrared spectroscopy gave discrepant water contents of 2300 ± 200 and 600 ± 12 ppm, respectively (Thiéblot et al. 1998; Hofmeister 1995). In any case, the hydrogrossular component should represent less than 3 mol%. The titanite sample was synthesized from a stoichiometric mix of TiO_2, SiO_2, and $CaCO_3$ powders dried at 1370, 1370, and 820 K, respectively. After decarbonation, the mix was melted at 1770 K in a platinum crucible and crystallized at 1270 K for 10 h. Powder X-ray diffraction (XRD) experiments were made after sample synthesis for grossular and titanite. In both cases, a single-phase

*Present Address: Musée de Minéralogie de l'Ecole des Mines de Paris (ENSMP), Paris, France.
†E-mail: richet@ipgp.jussieu.fr

pattern was obtained and gave, with the refinement program LCR2, unit-cell parameters in agreement with standard data (Table 1). For titanite, the unit cell parameters are consistent with the results reviewed by Xirouchakis et al. (1997a) for "subsolidus-derived" samples.

Single crystals of orthoenstatite were synthesized with the flux method described by Grandin de l'Eprevier (1972) and used by Ito (1975). The flux consisted of 90 g of Li_2CO_3, 140 g of MoO_5, and 25 g of V_2O_5 to which we added ~15 g of a stoichiometric mix of MgO and SiO_2 powders dried at 1370 K prior to weighing. To ensure complete dissolution of MgO and SiO_2 in the flux, the mixture was melted at 1200 K for 5 d in a platinum crucible in an electric muffle furnace. The temperature was then lowered to 920 K at a rate of 2 K/hour. Orthoenstatite single crystals were recovered through dissolution of the quenched material into distilled water. These crystals were nice 5 mm long needles elongated on *c*, but they represented only 20% of the enstatite material originally dissolved in the flux. We recovered the flux through evaporation of the aqueous solution and repeated the procedure after adding 15 g of another stoichiometric $MgO:SiO_2$ mix. About 12 g of crystalline material were eventually obtained, with a size ranging from 0.1 to 5 mm. As grinding induces partial transformation of ortho- to clinoenstatite (e.g., Lee and Heuer 1987), we could not use powder XRD to check the single phase nature of the material to be used for the calorimetric measurements. Instead, we sifted the run product and retained the 0.5–5 mm fraction, corresponding to orthorhombic single crystals that could be clearly identified under a binocular microscope. These were recovered in a pristine condition after the calorimetry measurements. Although the presence of small amounts of clinoenstatite after grinding was actually observed, the lattice parameters of this orthoenstatite sample could be determined from powder XRD experiments (Table 1). For measurements at higher temperatures on protoenstatite, we used another synthetic material made from MgO and quartz powders ground in an agate mortar and heated to 1920 K. The resulting melt was then cooled to 1620 K, annealed for 2 d, and finally quenched to room temperature.

Calorimetry measurements

About 5 g of the minerals were loaded as a fine or coarse powder in Pt-Rh 15% crucibles for drop-calorimetry experiments made with the procedures and the two different setups described by Richet et al. (1982, 1992) for measurements above and below 1000 K, respectively. After having been heated at a temperature *T*, which was measured with two thermocouples at the center of the crucible, the crucible was dropped into an ice calorimeter in which the relative enthalpy $H_T - H_{273}$ released was measured. The heating stage of the experiments lasted generally <1 h and complete cooling to 273 K after the drop took ~20 min. For both setups, measurements on α-Al_2O_3, the calorimetric standard, indicated instrumental inaccuracies of <0.2% for the relative enthalpies and of <0.5% for the heat capacities determined by differentiation of equations fitted to the relative enthalpies (Richet et al. 1982, 1992).

In preliminary experiments, we determined the maximum temperature that grossular could withstand without decomposing under heat treatments similar to those of the drop-calorimetry measurements. For this purpose, 200 mg of the material were heated for 30 min at a given temperature, quenched, and examined by optical microscopy and XRD. No signs of decomposition were detected below 1350 K. As decomposition began between 1400 K and 1500 K, these temperatures constituted the upper limit for relative enthalpy measurements. The XRD pattern of the sample recovered at the end of these measurements did not show signs of decomposition. This is consistent with our subsequent high-temperature XRD study where the onset of decomposition was detected at about 1460 K for a very finely ground powder of the same material (Thiéblot et al. 1998).

Previous studies have indicated that protoenstatite forms rapidly at high temperatures (Brown and Smith 1963; Murakami et al. 1982; Yang and Ghose 1995). Consistent with these findings, only protoenstatite reflections were observed in a series of XRD experiments made on this material from 1320 to 1820 K (Thiéblot 1996). In contrast to the single-phase nature of the sample before the drop, a complex polymorphic mixture was observed in an XRD pattern recorded on part of the sample after the calorimetric measurements. Although this was expected for samples heat treated in this way (Boysen et al. 1991), determining the proportions of the different polymorphs unfortunately was not possible because of the large size (~5 g) of the sample, the differences in cooling rate the sample experienced between its inner and outer parts, and the polymorphic changes induced by grinding the sample at room temperature. As demonstrated by Richet and Bottinga (1984), however, the rate at which a sample cools down in our calorimeter depends little on the temperature before the drop. This ensured a good reproducibility for the transformations undergone by protoenstatite on cooling to 273 K. Indeed, without such a reproducibility, the precision of the measured enthalpies would not have been as good for protoenstatite as for the other minerals.

TABLE 1. Room-temperature lattice parameters of the minerals

	a (Å)	*b* (Å)	*c* (Å)	β (°)	*V* (Å³)
Grossular*	11.8512 (6)				1664.5 (3)
Orthoenstatite†	18.230 (5)	8.820 (2)	5.176 (2)		832.2 (7)
Titanite‡	7.065 (5)	8.720 (5)	6.557 (4)	113.86 (5)	368.6 (12)

* Compare with *a* = 11.851 (1) Å as reported by Geiger et al. (1987).
† Compare with *a* = 18.225 (2), *b* =8.813 (1), *c* = 5.180 (1) Å and *V* = 832.0 (2) Å³ as given by Lee and Heuer (1987).
‡ Compare with *a* = 7.062 (1), *b* = 8.716 (2), *c* = 6.559 (1), β = 113.802 (1)° and *V* = 369.4 (3) Å³, as given by Xirouchakis et al. (1997a) for "subsolidus-derived" samples.

RESULTS AND DISCUSSION

Heat capacity determinations

The experimental relative enthalpies are listed in Table 2 where series and runs are labeled in chronological order and the suffix -B indicates measurements made with the lower-temperature setup. In the following, the enthalpy data also will be plotted in the form of mean heat capacities

$$C_m = (H_T - H_{273})/(T - 273). \quad (1)$$

This representation is especially useful because it provides a plot of the raw data at an expanded scale, without possible fitting bias. For all minerals a smooth variation of the mean heat capacity is observed, without any discontinuities or abrupt

TABLE 2. Relative enthalpy $H_T - H_{273}$ of grossular, ortho- and protoenstatites, and titanite (kJ/mol)

No.	T (K)	H_T-H_{273}	No.	T (K)	H_T-H_{273}
	Grossular			**Protoenstatite**	
ET11-B	407.7	48.11	EX17	1366.3	129.17
ET1-B	454.2	66.89	EX11	1427.1	136.84
ET14-B	540.1	103.62	EX4	1481.0	143.47
ET12-B	599.7	129.28	EX2	1574.6	155.98
ET6-B	639.2	147.74	EX3	1683.1	169.66
ET15-B	696.2	174.61	EX26	1739.9	177.16
ET3-B	751.9	200.51	EX16	1744.9	177.83
ET16-B	844.2	244.66	EX5	1773.2	182.56
ET4-B	907.7	274.99	EX15	1787.3	184.77
ET8-B	954.3	298.46	EX10	1811.4	191.86
ET5-B	997.7	319.37			
ET9-B	1043.8	342.84		**Titanite**	
ET21	1075.3	358.30	FG3-B	436.1	24.873
ET10	1133.8	387.83	FG6-B	542.7	43.253
ET22	1167.5	404.11	FG4-B	619.7	57.305
ET26	1226.7	433.38	FG9-B	711.8	74.416
ET24	1248.3	443.86	FG7-B	796.2	90.322
ET25	1350.3	495.93	FG13-B	1002.5	130.58
ET27*	1386.3	512.65	FG1	1085.4	146.98
			FG2	1177.9	165.21
	Orthoenstatite		FG5	1268.7	183.01
EE12-B	415.6	12.64	FG8	1365.8	202.94
EE1-B	513.7	22.87	FG11	1478.1	226.66
EE11-B	514.1	22.73	FG15	1530.6	238.06
EE4-B	638.5	36.54	FG17	1568.7	248.16
EE2-B	696.6	43.30	FG18	1592.6	255.80
EE20-B	724.1	46.75	FG19	1613.1	262.62
EE5-B	771.7	52.16	FG20	1631.9	272.98
EE13-B	849.6	61.70	FG21	1642.9	284.72
EE6-B	907.9	68.89	FG24	1648.5	293.92
EE8-B	968.4	76.51	FG22	1653.8	326.92
EE9-B	1051.8	86.96	FG23	1658.0	366.75
EE10-B	1168.6	101.85	FG28	1707.9	335.00*
EE17	1225.4	109.51			

* Product overflow during the drop.

changes in the slope of the C_m curves.

To determine heat capacities, we made least-squares fits to the experimental relative enthalpy data

$$H_T - H_{273} = R_{273} + \int_{273}^{T} C_p \, dT \qquad (2)$$

which we differentiated with respect to temperature. In Equation 2, the constant R_{273} was an adjustable parameter for protoenstatite only, being determined by the constraint $H_T - H_{273} = 0$ for the other minerals. Various kinds of empirical C_p equations were used in these fits. The well-known Haas and Fisher (1976) equation is given by:

$$C_p = a + bT + c/T^2 + d/T^{0.5} + eT^2. \qquad (3)$$

We also used equations of the form recommended for high-temperature extrapolations by Berman and Brown (1985):

$$C_p = k_0 + k_{0.5}/T^{0.5} + k_2/T^2 + k_3/T^3 \qquad (4)$$

and by Richet and Fiquet (1991):

$$C_p = k_0 + k_{\ln} \ln T + k_1/T + k_2/T^2 + k_3/T^3. \qquad (5)$$

None of these equations are flexible enough to reproduce the enthalpy anomalies that can be observed near the melting point. Consquently, we used the following expression, as done previously by Richet et al. (1994):

$$C_p = A\,(1 - T/T_f)^{-\alpha} + a + bT + c/T^2 + d/T^{0.5} + eT^2 \qquad (6)$$

where T_f is the melting temperature and $A\,(1 - T/T_f)^{-\alpha}$ is an extra term added to account for the very steep C_p increase in phase transition regions.

Grossular

The relative enthalpy of grossular was measured previously by Kiseleva et al. (1972). Their results on a natural sample, plotted in Figure 1 in the form of mean heat capacities, deviate by up to 1% from our results. As obtained from a fit made with Equation 3 to our data only (Fig. 2), our heat capacities agree to within ±1% with the differential scanning calorimetry (DSC) observations of Perkins et al. (1977) and Bosenick et al. (1996). These differences are well within the error margins of the techniques, and are indeed similar to those found between the results of Bosenick et al. (1996) and the measurements from our laboratory for pyrope and MgO (Téqui et al. 1991; Richet and Fiquet 1991). The other DSC observations of Krupka et al. (1979) for a natural and a synthetic sample differ surprisingly by up to 5% from these results, lying on both sides of them. Inasmuch as the high-temperature heat capacity of solids generally depends very little on impurity content, the reason for this discrepancy was unknown to Krupka et al. (1979). By infrared spectroscopy (Hofmeister, personnal communication), it has been found that this synthetic sample contained about 0.7 ± 0.1 wt% H_2O, but this fact does not account readily for the anomalous scatter data of Krupka et al.

At low temperatures, three different sets of adiabatic measurements (Krupka et al. 1979; Westrum et al. 1979; Haselton and Westrum 1980) show unusual differences that cannot be explained in terms of impurity content or natural vs. synthetic samples. The results of Kolesnik et al. (1979) for a pure natural sample are 3% lower than those of Westrum et al. (1979) below 80 K and become 1% higher above 150 K. The measurements of Westrum et al. (1979) join smoothly with ours above room temperature, whereas those of Haselton and Westrum (1980) tend to be slightly too high above 300 K. The coeffi-

TABLE 3. Coefficients of heat capacity equations (J/mol·K)*

	Eq. 3					Eq. 4			
	a	10^3b	10^{-5}c	d	AAD†	k_0	$k_{0.5}$	$10^{-6}k_2$	AAD
Grossular	787.356	–63.840	–16.107	–7235.0	0.24	620.741	–3580.8	–7.032720	0.17
Orthoenstatite	201.585	–11.933	0.46073	–2011.5	0.11	175.937	–1535.4	–0.438856	0.14
Protoenstatite‡	115.752	8.2071			0.06				
Titanite	358.276	–45.276	11.488	–3723.4	0.07	222.937	–722.42	–3.846450	0.11

* Fits up to 1683 K and 1269 K with Equations 3–5 for protoenstaite and titanite, respectively, and up to the highest temperatures for both phases with Equation 6.
† Average absolute deviation of the fitted from the experimental values of Table 2.
‡ R_{273} = –36.712, 1.747, and 51.105 106 kJ/mol for Equations 3, 5, and 6, respectively.

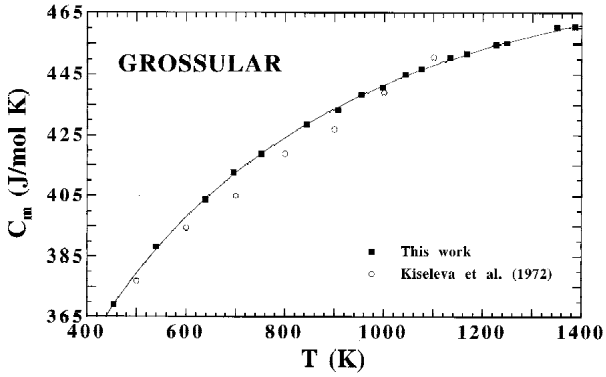

FIGURE 1. Mean heat capacity of grossular. Experimental $H_T - H_{273}$ data of Kiseleva et al. (1972, open circles; referred with Eq. 3 to 273.15 K) and this work (solid squares), and fitted values as given by Equation 3 and the data of Table 4 (solid curve).

cients of the various C_p equations reported in Table 3 have thus been obtained from least-squares fits made simultaneously to the C_p data of Westrum et al. (1979), above 273 K, and Bosenick et al. (1996), and to our relative enthalpies. All these equations reproduce in nearly the same way the input data, with average absolute deviations (AAD) of the fitted values from the experimental data of 0.16, 0.19, and 0.24% for Westrum et al. (1979), Bosenick et al. (1996), and this work, respectively, and 0.76% for those of Haselton and Westrum (1980).

An unexpected feature of the high-temperature heat capacity of grossular is an anomalously slight temperature dependence (Fig. 3), which appears in our data above ~1200 K, i.e., at the upper end of our calorimetric measurements. This finding is at variance with the values calculated from vibrational modeling by Hofmeister and Chopelas (1991), with the empirical values given by Berman (1988), and with the smooth C_p increase exhibited by pyrope up to very high temperatures (Téqui et al. 1991). In fact, this discrepancy is especially intriguing, as high-temperature XRD experiments on the same material have yielded a "normal" thermal expansion coefficient of 2.7 (3)/K at 1400 K, for instance (Thiéblot et al. 1998), which agrees with the value of 2.9/K used by Hofmeister and Chopelas (1991) at this temperature to derive isobaric heat capacities from the calculated isochoric values. Anomalous changes in the frequencies of vibrational modes accounting for this behavior could be sought through Raman or infrared spectroscopy measurements up to the highest temperatures achieved in this study.

Enstatites

As found previously for several other materials (e.g., Richet et al. 1982; Richet and Fiquet 1991), our data are consistent with the relative enthalpies measured by White (1919; see Fig. 4). Our data also agree with those of Stebbins et al. (1984) between 1650 and 1800 K whereas the results of Wagner (1932) are systematically lower than ours, for example by ~4% at 1200 K—a much greater difference than previously noted between the results of both laboratories (Richet and Fiquet 1991). In view of the apparently slight heat capacity differences between enstatite polymorphs discussed below, this discrepancy does not seem to be accounted for in terms of the different forms investigated. Our results agree well with the DSC orthoenstatite measure-

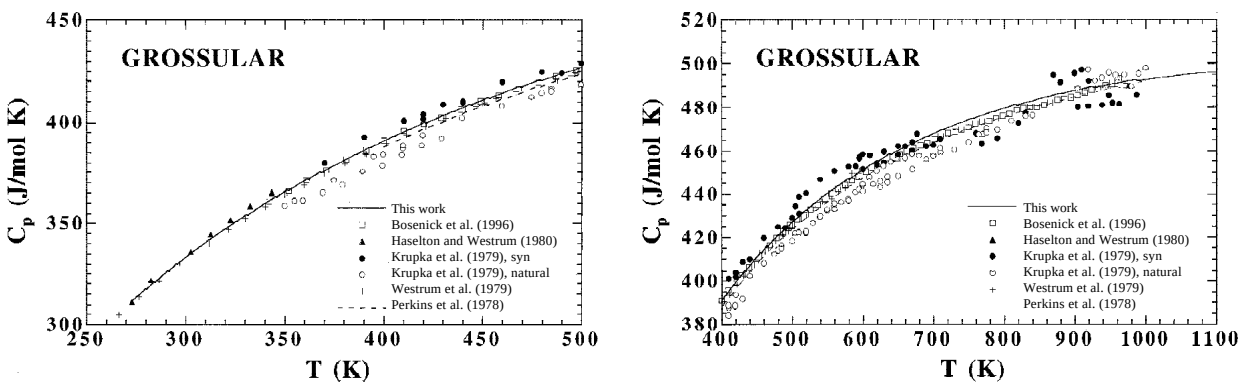

FIGURE 2. (**left** and **right**). Heat capacity of grossular: experimental data and fitted values (solid curve) as given by Equation 3.

TABLE 3. —*Extended*

Eq. 5				Eq. 6							
K_0	K_{ln}	$10^{-3}k_1$	AAD	A	α	a	b	10^{-5} c	d	10^4 e	AAD
955.695	–52.741	99.109	0.17								
50.873	12.809	–12.459	0.14								
41.947	12.242	–4.9604	0.10	0.2240	–1.308	129.0		–51.105		0.11	
355.865	–18.254	–33.724	0.10	1.4405	–1.493	134.7	0.1375	–1.101	–366.6	–0.688	0.12

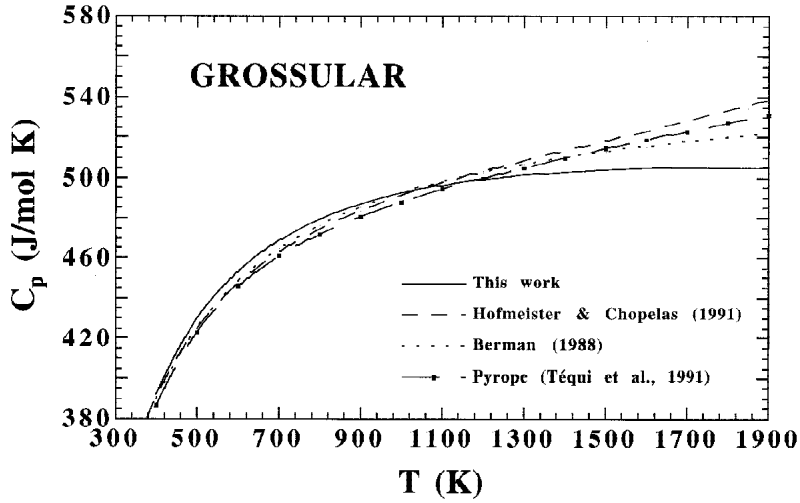

FIGURE 3. High-temperature extrapolations of the heat capacity of grossular. The data of Téqui et al. (1991) for pyrope have been included for comparison.

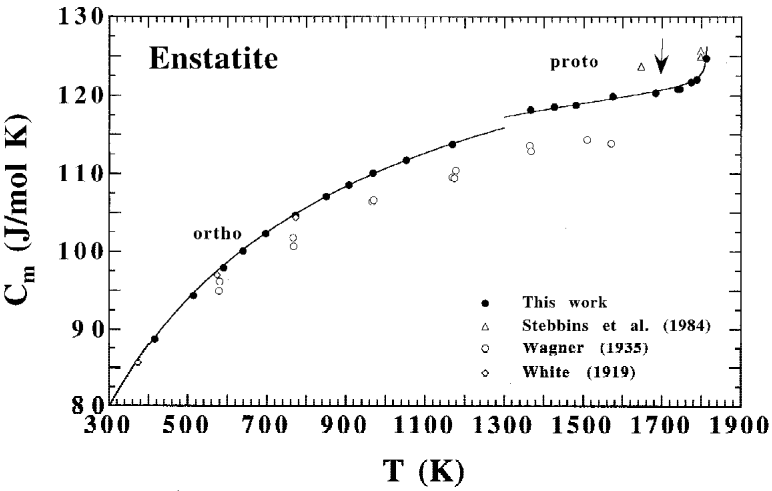

FIGURE 4. Mean heat capacities of ortho–enstatite and protoenstatite: experimental data of Table 2 and fitted values as given by Equations 3 and 6, respectively. The discontinuity at around 1300 K represents an enthalpy of partial conversion of protoenstatite to lower-temperature polymorphs (see text). The arrow indicates the onset of premelting.

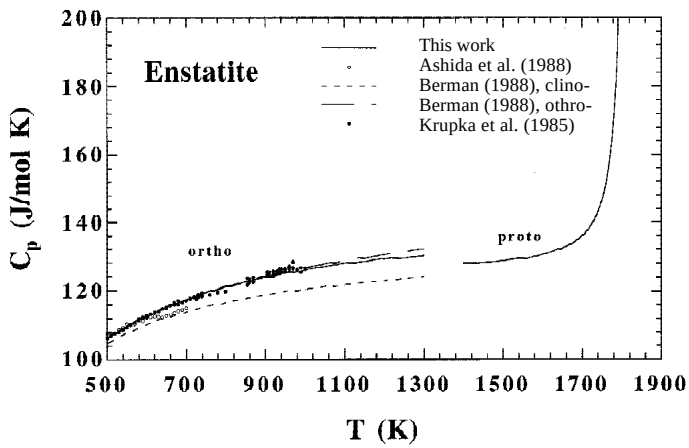

FIGURE 5. Heat capacities of ortho- and protoenstatite. Experimental data and values given by Berman (1988) and by Equations 3 and 6 for ortho- and protoenstatite, respectively.

ments of Watanabe (1982) and Krupka et al. (1985) up to 800 K above which the latter show a greater scatter. As a matter of fact, these results and ours were reproduced to within 0.11, 0.14, and 0.14%, respectively, with the C_p equations of Table 3. The consistency is less good for other DSC data by Ashida et al. (1988), which deviate on the average by 2% from our recommended values above 650 K (Fig. 5).

At 1 bar the temperatures of the ortho-clino and clino-protoenstatite transitions are 870 and 1300 K, respectively (Lee and Heuer 1987). For orthoenstatite, our measurements thus extend markedly into the stability field of the monoclinic form. We have already noted that, consistent with both a transmission electron microscopy study (Shimobayashi and Kitamura 1993) and the calorimetric results (Fig. 4), inspection of the material at the end of the experiments with a binocular microscope did not show evidence of partial transformation.

For protoenstatite, the experiments were made from 1366 K on a finely powdered sample. During the heating stage of the experiments, the kinetics of the transformation of ortho- or clinoenstatite was rapid enough that protoenstatite actually formed (cf. Brown and Smith 1963; Murakami et al. 1982; Yang and Ghose 1995). That protoenstatite was not wholly preserved on cooling in the calorimeter, in contrast, is clearly shown by the apparent discontinuity of about 2 kJ/mol observed between the enthalpy curves of "proto-" and orthoenstatite near 1300 K (Fig. 4). If protoenstatite had transformed completely to either ortho- or clinoenstatite, this value would represent its enthalpy of transition to lower temperature polymorphs. From phase equilibria data, Gasparik (1990) determined enthalpies of transition of about 9 and 11 kJ/mol for proto- to ortho- and clinoenstatite, respectively. Hence, either these values are too high or, more likely, only part of our protoenstatite sample actually reverted to other forms on cooling to 273 K. This outcome would be consistent with the complex nature of quenched protoenstatite samples, which depends on several factors, such as cooling rates or sample purity, through stacking faults and a strong sensitivity to shear (Brown and Smith 1963; Smyth 1974; Schrader et al. 1990; Boysen et al. 1991).

As already noted, the important fact is that the good reproducibility of the measurements in the protoenstatite stability field indicates that the nature and mineral proportion of the final product at 273 K did not depend sensitively on the temperature from which the sample was quenched. This justifies determining the heat capacity of protoenstatite from the measured relative enthalpies. In this respect, it is unlikely fortuitous that the high-temperature extrapolation of the heat capacity of orthoenstatite differs by less than 3% from the heat capacity of protoenstatite at the low end of its stability field (Fig. 5). Not unexpectedly, the relatively minor density differences between the polymorphs do not translate into markedly different heat capacities at high temperatures. By analogy, these data suggest that the heat capacity of clinoenstatite should not differ much from the values reported here for orthoenstatite, and the same conclusion could also apply to high-pressure clinoenstatite. On the other hand, this conclusion could seem inconsistent with the C_p difference indicated by the data of Berman (1988) for clino and orthoenstatite (Fig. 5). Note, however, that the equation of Berman (1988) for clinoenstatite was derived from the observations of Wagner

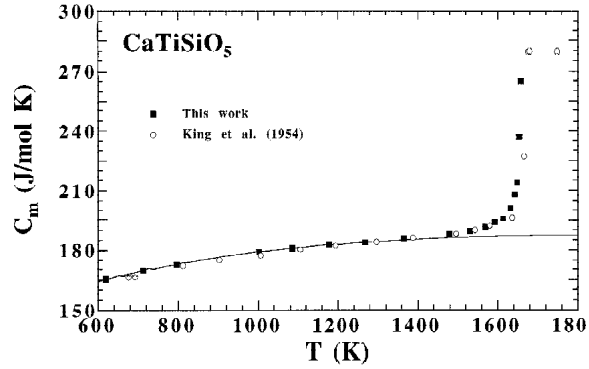

FIGURE 6. Mean heat capacity of titanite. Experimental data of King et al. (1954, open circles) and this work (solid squares).

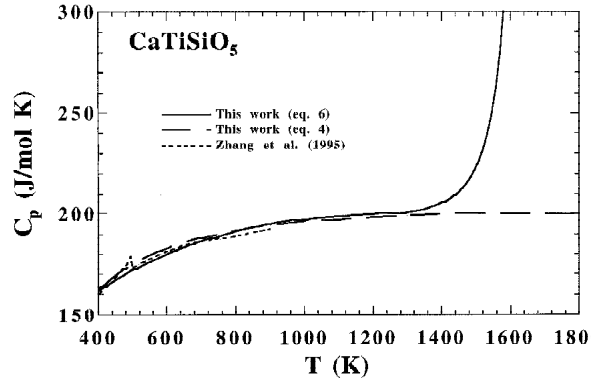

FIGURE 7. Heat capacity of titanite as determined by King et al. (1954), Zhang et al. (1995), and in this work.

(1932) who did not give any detail regarding the characterization of his "clinoenstatite" sample.

Another noteworthy feature seen in Figure 5 is the anomalous enthalpy increase due to premelting that begins near 1700 K, i.e., 130 K below the onset of incongruent melting of protoenstatite (Boyd et al. 1964), which translates to a very steep heat capacity gradient. From their high-pressure experiments, Boyd et al. (1964) could not resolve to better than 20 K the 1-bar metastable, congruent melting point of protoenstatite from its actual solidus. This temperature of congruent melting has to be lower than the solidus, and we indeed found that a critical temperature of about 1816 K in Equation 6 allowed us to optimize the fit to the data of Table 2. The difference between the heat capacities given by Equations 6 and 5 indicates that the enthalpy of premelting (between the temperature of the onset of premelting and the metastable, congruent melting temperature of 1816 K) is about 7 kJ/mol and thus represents about 10% of the enthalpy of fusion of 73 ± 6 kJ/mol (Richet and Bottinga 1986). This fraction thus appears to be somewhat lower than the 17% determined previously for diopside and pseudowollastonite (Richet et al. 1994), two other minerals with a pyroxene stoichiometry. For both of these minerals, the onset of premelting correlates with an enhanced dynamics of the alkaline earth cations (Dimanov and Ingrin 1995; Richet et al. 1998). Regardless of the precise nature of the dynamics at work in premelting, this suggests that

a slightly stronger bonding makes it somewhat less effective in enstatite than in Ca-bearing phases.

Titanite

Our measurements are in excellent agreement (Fig. 6) with the results of King et al. (1954) which have long represented the only calorimetric information available. Recently, C_p data reported graphically (Zhang et al. 1995) have shown a slight lambda-type anomaly for the para-antiferroelectric transition observed near 500 K (Fig. 7). Owing to its low temperature and small enthalpy of ~80 J/mol, this transition is not apparent in the drop-calorimetry data. Likewise, the calorimetric effects of the phase transitions reported at 825 K and possibly near 1150 K (Zhang et al. 1997; Chrosch et al. 1997) also appear too small to be detected from relative-enthalpy measurements. For practical purposes, we thus list in Table 3 C_p equations valid from room up to high temperatures. With Equation 3, for example, the data of King et al. (1954) and Table 2 are on the average reproduced to within 0.07 and 0.10%, respectively. Besides, Xirouchakis et al. (1997a, 1997b) have pointed out that the lattice parameters and enthalpy of formation of titanite depend on synthesis conditions. Heat capacities, in contrast, are in general much less sensitive to minor structural differences. This is borne out by the good agreement between our results and previous data because the sample investigated by King et al. (1954) crystallized from a melt and, according to the summary shown by Xirouchakis et al. (1997a), should have had lattice parameters differing from those of our own sample.

The onset of premelting has been observed near 1550 K by King et al. (1954) and in this study as well, i.e., about 110 K below the congruent melting point. In Table 3, the coefficients of Equation 6 have been determined from data extending up to 1643 K. They give an enthalpy of premelting of about 30 kJ/mol, but this estimate is not well constrained because the actual limit between premelting and melting is difficult to pinpoint. As titanite is not a glass former and instead crystallizes readily from the melt on cooling, King et al. (1954) could measure directly the enthalpy of fusion as 124 kJ/mol. Our intent was to check this result, but the very high fluidity of the melt prevented us from doing so. Our measurements point to a slightly lower melting temperature than previously reported, namely about 1658 ± 3 K instead of 1665 ± 5 K, in agreement with the range 1648-1656 K found through differential thermal analysis by Crowe et al. (1986).

Although different samples were investigated, the agreement between our results and those of King et al. (1954) is especially noteworthy when the melting point is being approached. Once more, this confirms that premelting is an intrinsic feature of a crystal that does not depend on some sample peculiarity. Titanite is made up of chains of corner-sharing TiO_6-octahedra whose cross-linking by SiO_4-tetrahedra delineate large sites where Ca is sevenfold coordinated (Taylor and Brown 1976). It would be interesting to determine whether premelting is associated mainly with an enhanced mobility of Ca, as found for diopside and pseudowollastonite, or if the distinct structural roles played by Si, Ti, and Ca can give rise to a more complex behavior. Finally, it has been pointed out that no premelting is observed for minerals such as quartz (SiO_2) or carnegieite ($NaAlSiO_4$), which experience α-β transitions giving rise to high-temperature phases with dynamically averaged structures (Richet et al. 1994). This is not the case of the transitions experienced by titanite, as revealed by their very small enthalpies, whence the observation of typical premelting effects.

Acknowledgements

This work was part of an NSF-CNRS cooperative research program between the University of California at Davis (A.M. Hofmeister) and IPGP (P. Richet). We thank A. Bosenick and C.A. Geiger for communicating data, W.L. Brown for discussion, M.A. Bouhifd for comments, and A. Bosenick and D. Xirouchakis for thorough reviews.

References cited

Ashida, T., Kume, S., Ito, E., and Navrotsky, A. (1988) $MgSiO_3$ ilmenite: heat capacity, thermal expansivity, and enthalpy of transformation. Physics and Chemistry of Minerals, 16, 239–245.

Berman, R.G. (1988) Internally consistent thermodynamic data for minerals in the system Na_2O-K_2O-CaO-MgO-FeO-Fe_2O_3-Al_2O_3-SiO_2-TiO_2-H_2O-CO_2. Journal of Petrology, 29, 445–522.

Berman, R.G. and Brown, T.H. (1985) Heat capacity of minerals in the system Na_2O-K_2O-CaO-MgO-FeO-Fe_2O_3-Al_2O_3-SiO_2-TiO_2-H_2O-CO_2: representation, estimation and high temperature extrapolation. Contributions to Mineralogy and Petrolology, 89, 168–183.

Bosenick, A., Geiger, C.A., and Cemic, L. (1996) Heat capacity measurements of synthetic pyrope-grossular garnets between 320 and 1000 K by differential scanning calorimetry. Geochimica et Cosmochimica Acta, 60, 3215–3227.

Boyd, F.R., England, J.L., and Davis, B.C. (1964) Effects of pressure on the melting and polymorphism of enstatite, $MgSiO_3$. Journal of Geophysical Researchs, 69, 2101–2109.

Boysen, H., Frey, F., Schrader, H., and Eckold G. (1991) On the proto- to orthoclino enstatite phase transformation: single crystal X-ray and inelastic neutron investigation. Physics and Chemistry of Minerals, 17, 629–635.

Brown, W.L. and Smith, J.V. (1963) High-temperature X-ray studies on the polymorphism of $MgSiO_3$. Zeitschrift für Kristallographie, 118, 186-212.

Chrosch, J., Bismayer, U., and Salje, E.K.H. (1997) Anti-phase boundaries and phase transitions in titanite: An X-ray diffraction study. American Mineralogist, 82, 677–681.

Crowe, M.C., Greedan, J.E., Garrett, J.D., Burke, N.A., Vance, E.R., and George, I.M. (1986) Melt-grown sphene ($CaTiSiO_5$) crystals. Journal of Material Science Letters, 5, 979–980.

Dimanov, A. and Ingrin, J. (1995) Premelting and high temperature diffusion of Ca in synthetic diopside: an increase of the cation mobility. Physics and Chemistry of Minerals, 22, 437–442.

Gasparik, T. (1990) A thermodynamic model for the enstatite-diopside join. American Mineralogist, 75, 1080–1091.

Geiger, C.A., Newton, R.C., and Kleppa, O.J. (1987) Enthalpy of mixing of synthetic almandine-grossular and almandine-pyrope garnets from high-temperature solution calorimetry. Geochimica et Cosmochimica Acta, 51, 1755–1763.

Ghose, S., Ito, Y., and Hatch, D.M. (1991) Paraelectric-antiferroelectric phase transition in titanite, $CaTiSiO_5$. Physics and Chemistry of Minerals, 17, 591–603.

Grandin de l'Eprevier (1972) Synthèse de monocristaux de forstérite, Mg_2SiO_4 par la méthode des sels fondus. Thèse, Faculté des Sciences, Orléans, France, 56 p.

Haas, J.L. and Fisher, J.R. (1976) Simultaneous evaluation and correlation of thermodynamic data. American Journal of Science, 276, 525–545.

Haselton, H.T. and Newton, R.C. (1980) Thermodynamics of pyrope-grossular garnets and their stabilities at high temperatures and high pressures. Journal of Geophysical Researchs, 85, 6976–6982.

Haselton, H.T. and Westrum, E.F. (1980) Low-temperature heat capacities of synthetic pyrope, grossular, and $pyrope_{60}$ $grossular_{40}$. Geochimica et Cosmochimica Acta, 44, 701–709.

Hofmeister, A.M. (1995) Infrared microspectroscopy. In H.J. Humecki, Ed., Practical Guide to Infrared Spectroscopy, 2nd ed., p. 377–416. Marcel Dekker, New York.

Hofmeister, A.M. and Chopelas, A. (1991) Thermodynamic properties of pyrope and grossular from vibrational spectroscopy. American Mineralogist, 76, 880–891.

Ito, J. (1975) High-temperature solvent growth of orthoenstatite, $MgSiO_3$, in air. Geophysical Research Letters, 2, 533–536.

King, E.G., Orr, R.L., and Bonnickson, K.R. (1954) Low-temperature heat capacity, entropy at 298.16 K, and high temperature heat content of sphene ($CaTiSiO_5$). Journal of the American Chemical Society, 76, 4320–4321.

Kiseleva, I.A., Topor, N.D., and Mel'chakova, L.V. (1972) Experimental determination of heat content and heat capacity of grossularite, andradite and pyrope. Geokhimiya, 1372–1379.

Kolesnik, Y.N., Nogteva, V.V., Arkhipenko, D.K., Orekhov, B.A., and Paukov, I.E. (1979). Thermodynamics of pyrope-grossular solid solutions and the specific heat of grossular at 13–300 K. Geokhimiya, 5, 713–721.

Krupka, K.M., Robie, R.A., and Hemingway, B.S. (1979) High-temperature heat capacities of corundum, periclase, anorthite, $CaAl_2Si_2O_8$ glass, muscovite, pyrophillite, $KAlSi_3O_8$ glass, grossular, and $NaAlSi_3O_8$ glass. American Mineralogist, 64, 86–101.

Krupka, K.M., Robie, R.A., Hemingway, B.S., Kerrick, D.M., and Ito, J. (1985) High-temperature heat capacities and derived thermodynamic properties of anthophyllite, diopside, enstatite, bronzite and wollastonite. American Mineralogist, 70, 261–271.

Lee, W.E. and Heuer, A.H. (1987) On the polymorphism of enstatite. Journal of the American Ceramic Society, 70, 349–359.

Murakami, T., Takeuchi, Y., and Yamanaka, T. (1982) The transition of orthoenstatite to protoenstatite and the structure at 1080 °C. Zeitschrift für Kristallographie, 160, 299–312.

Perkins, D., III, Essene, E.J., Westrum, E.F. Jr., and Wall, V.J. (1977) Application of new thermodynamic data to grossular phase relations. Contributions to Mineralogy and Petrolology, 64, 137–147.

Richet, P. and Bottinga, Y. (1984) Glass transitions and thermodynamic properties of amorphous SiO_2, $NaAlSi_nO_{2n+2}$ and $KAlSi_3O_8$. Geochimica et Cosmochimica Acta, 48, 453–470.

——— (1986) Thermochemical properties of silicate glasses and liquids: a review, Reviews of Geophysics, 24, 1–25.

Richet, P. and Fiquet, G. (1991) High-temperature heat capacity and premelting of minerals in the system MgO-CaO-Al_2O_3-SiO_2. Journal of Geophysical Research, 96, 445–456.

Richet, P., Bottinga, Y., Deniélou, L., Petitet, J.P., and Téqui, C. (1982) Thermodynamic properties of quartz, cristobalite and amorphous SiO_2: drop calorimetry measurements between 1000 and 1800 K and a review from 0 to 2000 K. Geochimica et Cosmochimica Acta, 46, 2639–2658.

Richet, P., Gillet, P., and Fiquet, G. (1992) Thermodynamic properties of minerals: macroscopic and microscopic approaches. Advances in Physical Geochemistry, 10, 98–131.

Richet, P., Ingrin, J., Mysen, B.O., Courtial, P., and Gillet, P. (1994) Premelting of minerals: an experimental study, Earth and Planetary Science Letters, 121, 589–600.

Richet, P., Mysen, B.O., and Ingrin, J. (1998) High-temperature X-ray diffraction and Raman spectroscopy of diopside and pseudowollastonite, Physics and Chemistry of Minerals, 25, 401–414.

Schrader, H., Boysen, H., Frey, F., and Convert, P. (1990) On the phase transformation proto- to clino-/orthoenstatite: neutron powder investigation. Physics and Chemistry of Minerals, 17, 409–415.

Shimobayashi, N. and Kitamura, M. (1993) Phase transition of orthoenstatite to high-clinoenstatite: *in situ* TEM study at high temperatures. Mineralogical Magazine, 16, 416–426.

Smith, J.V. (1969) Crystal structure and stability of the $MgSiO_3$ polymorphs; physical properties and phase relations of Mg,Fe pyroxenes. Mineralogical Society of America Special Paper, 2, 3–29.

Smyth, J.R. (1974) Experimental study of the polymorphism of enstatite. American Mineralogist, 59, 345–352.

Stebbins, J.F., Carmichael, I.S.E., and Moret, L.K. (1984) Heat capacities and entropies of silicate liquids and glasses. Contributions to Mineralogy and Petrolology, 86, 131–148.

Taylor, M. and Brown, G.E., Jr. (1976) High-temperature structural study of the $P2_1/a$=$A2/a$ phase transition in synthetic titanite, $CaTiSiO_5$. American Mineralogist, 61, 435–447.

Téqui, C., Robie, R.A., Hemingway, B.S., Neuville, D.R., and Richet, P. (1991) Melting and thermodynamic properties of pyrope ($Mg_3Al_2Si_3O_{12}$). Geochimica et Cosmochimica Acta, 55, 1005–1010.

Thiéblot, L. (1996) Etude des propriétés thermodynamiques de l'enstatite et des grenats à haute température, et de la préfusion. Thèse, Université Paris 7, 197 p.

Thiéblot, L., Roux, J., and Richet, P. (1998) High-temperature thermal expansion and decomposition of garnets. European Journal of Mineralogy, 10, 7–15.

Wagner, H. (1932) Zur Thermochemie der Metasilikate des Calciums und Magnesiums und des Diopsids. Zeitschrift für Anorganische und Allgemeine Chemie, 208, 1–28.

Watanabe, H. (1982) Thermochemical properties of synthetic high-pressure compounds relevant to the earth's mantle. In S. Akimoto and M.H. Manghnani, Eds., High-pressure Research in Geophysics, p. 441–464. Reidel, Dordrecht, The Netherlands.

Westrum, E.F., Jr., Essene, E.J., and Perkins, D., III (1979) Thermophysical properties of the garnet, grossular: $Ca_3Al_2Si_3O_{12}$. Journal of Chemical Thermodynamics, 11, 57–66.

White, W. P. (1919) Silicate specific heats. American Journal of Science, 47, 1–43.

Xirouchakis, D., Kunz, M., Parise, J.B., and Lindsley, D.H. (1997a) Synthesis methods and unit-cell volume of end-member titanite ($CaTiOSiO_4$). American Mineralogist, 82, 748–753.

Xirouchakis, D., Fritsch, S., Putnam, R. L., Navrotsky, A., and Lindsley, D.H. (1997b) Thermochemistry and the enthalpy of formation of end-member titanite ($CaTiSiO_5$). American Mineralogist, 82, 754–759.

Yang, H. and Ghose, S. (1995) High-temperature single-crystal X-ray diffraction studies of the ortho-proto phase transition in enstatite at 1360 K. Physics and Chemistry of Minerals, 22, 300–310.

Zhang, M., Salje, E.K.H., Bismayer, U., Unruh, H.G., Wruck, B., and Schmidt, C. (1995) Phase transition(s) in titanite $CaTiSiO_5$: an infrared spectroscopic, dielectric response and heat capacity study. Physics and Chemistry of Minerals, 22, 41–49.

Zhang, M., Salje, E.K.H., and Bismayer, U. (1997) Structural phase transition near 825 K in titanite: evidence from infrared spectroscopic observation. American Mineralogist, 82, 30–35.

MANUSCRIPT RECEIVED MARCH 30, 1998
MANUSCRIPT ACCEPTED DECEMBER 7, 1998
PAPER HANDLED BY J. WILLIAM CAREY